International Journal of Chemical Studies

P-ISSN 2349–8528
E-ISSN 2321–4902
IJCS 2014; 2(4): 10-19

Received: 11-10-2014
Accepted: 19-11-2014

M. N. Kouraim
Nuclear Materials Authority, P.O. Box 530, El Maadi, Cairo, Egypt.

N. M. Farag
Nuclear Materials Authority, P.O. Box 530, El Maadi, Cairo, Egypt.

S. A. Sadeak
Chemistry department, Faculty of Science, Zaggaziag University.

M. A. Gado
Nuclear Materials Authority, P.O. Box 530, El Maadi, Cairo, Egypt.

Correspondence:
M. N. Kouraim
Nuclear Materials Authority, P.O. Box 530, El Maadi, Cairo, Egypt.

Extraction of uranium using impregnated hydrophobic water hyacinth roots

M. N. Kouraim, N. M. Farag, S. A. Sadeak, M. A. Gado

Abstract
In this work, water hyacinth root (WHR) was directed to produce different modified adsorbents. The first (GWHR) was based on the graft copolymerization of vinyl-type monomers onto the backbone of WHR. The other adsorbents (TBP-WHR and TBP-GWHR) were prepared by the impregnation of the WHR by Tri butyl phosphate (TBP). Adsorbents characterization carried out using scanning electron microscope (SEM) and FT-IR. It was observed that adsorption capacities of the modified WHR are significantly greater than the conventional one. The adsorption capacity was found to be 42, 74, 153 and 400 mg g^{-1} for WHR, GWHR, TBP-WHR and TBP-GWHR, respectively.

Keywords: Extraction, Uranium, Impregnated, Hydrophobic, Water hyacinth roots

1. Introduction
Uranium is one of the most hazardous metals due to its high toxicity, as well as its radioactivity [1]. Among such traditional methods of uranium removal described before as, adsorption [2], coagulation [3] and membrane separation [4] the first one was considered as the most effective. Adsorbents as gibbsite [5], synthetic and natural zeolites [6, 7], composite ion exchangers [8], activated clay [9], chitosan [10] and biological sorbents [11] were used in practice for uranium removal. Being a low-cost material, water hyacinth root (WHR) seemed to have been one of the most perspective adsorbents taking into account its ability for removal of heavy metals from wastewater [12]. Adsorption of uranium from aqueous solutions by WHR was studied [13]. It was reported that OH groups and oxygen bridges of the WHR surface act as adsorption sites, forming hydrogen bonds with the uranium [14]. However, it suffers from lower selectivity and mass transfer rate. Different methods of WHR modification allowing increased its adsorption properties were described. Among these, the immobilization of selective solvents into its surface, where the solvent was retained on the internal surface of hydrophobic nonionic roots by adsorption rather than chemical bonding [15, 16]. Tributyl phosphate (TBP) was the most selective ligand used commercially, which also resists the strong oxidation action, so it is satisfactory for uranium extraction from nitrate aqueous solution media [17]. The tributyl phosphate impregnated resin shows a lower solubility in water as well as in nitrate solutions than in the liquid state. In this regard, the solubility of TBP in water is 0.38 g/L while its solubility in a polymeric resin support varies from an undetectable amount (0.02 g/L) to 0.2 g/L. Losses of TBP from the impregnated resins are negligible in relatively concentrated salt solutions, particularly in the acidic range [18–20].
However, the lignocelluloses materials originally existed in WHR are polar and hydrophilic. This renders them low susceptible to absorb TBP. One possible solution to this limitation could be the enhancement of the surface energy of lignocelluloses materials. Surface treatment can be occurred by introducing hydrophobic moieties onto the lignocelluloses backbone of WHR, for instance, by graft copolymerization of vinyl-type monomers onto the backbone. Graft copolymerization in the process of the study, in principle, comprises three different steps: initiation, propagation and termination. In this process, free radicals were generated for forming interfacial strong bonding such as covalent bonds between the roots and the polymerizable material or monomer. Surface modification can potentially enhance the compatibility of lignocelluloses materials with TBP in related applications.
This work involves preparation of hydrophobic water hyacinth roots (GWHR) and the TBP impregnation of either water hyacinth roots (TBP-WHR), or grafted roots (TBP-GWHR) as well as the extraction of uranium using these sorbents.

2. Experimental

2.1. Characterization of the uranium leach liquor

The studied uranium leach liquor used in this work was obtained from the dissolution of the uranium ore come from El-aluga, Sinai aria, Egypt. The ore was crushed to + 250 µm and then ground to the required particle size of (- 80 µm). The sample was first digested using complete attack method in which 1 g of sample was mixed with a mixture of conc. 10 mL HNO_3, 10 mL HF and 5 mL $HClO_4$ in Teflon beaker, was heated until dryness after that 5 ml of 50 % HNO_3 was added then completed to the required volume. The chemical compositions of ore and the leach liquor are listed in Table 1.

Table 1: Chemical analysis of the uranium ore and the applied leach liquor (weight %).

Component	El-aluga, Sinai ore	Leach liquor
SiO_2	62.16	----
Al_2O_3	06.30	01.30
TiO_2	00.37	00.05
Fe_2O_3	05.40	00.87
CaO	12.08	02.10
MgO	10.50	01.76
Na_2O	00.06	00.01
K_2O	00.45	00.12
P_2O_5	0.025	0.007
Uranium	2500 ppm	500 ppm

2.2. Chemicals and reagents

All chemicals and reagents used were of analytical grade. Uranium solutions were prepared using uranyl nitrate hexahydrate, $(UO_2)(NO_3)_2 .6H_2O$ (BDH, England). Analytical grade nitric acid solution (BDH, England) was used, and tributyl phosphate (TBP) was obtained from Merck. Kerosene (non-aromatic) was purchased from Misr for Petroleum Company. Uranium ions were standardized and measured spectrophotometrically as reported elsewhere [21]. The measurements were made with a Schimadzu UV-VIS-160 double beam spectrophotometer.

2.3. Preparation of the grafted water hyacinth roots (GWHR)

Air-dried water hyacinth roots are disintegrated in boiling deionized water under vigorous stirring for 30 minutes. The roots are filtered off, washed several times with water until obtaining a colorless clear solution. In a sealed 500 mL Erlenmeyer flask, an equivalent of 1.0 g oven dried roots (4 g wet) is suspended in 100 mL of water. 0.6 mL of concentrated nitric acid is after that added, and the slurry is deoxygenated by bubbling nitrogen flow through it for 30 minutes, while mixing vigorously in order to obtain well dispersed suspension. Ferrous ammonium sulfate hexahydrate (51 mg, 1.3 mmol/L) is later added to the root slurry, followed by 0.75 mL of a 34-37% aqueous hydrogen peroxide (0.25 % v/v). Five minutes later, 3.0 mL of methyl methacrylate (3.0 % v/v) is added to the pulp slurry and the reaction mixture is heated to 60° C. for one hour under vigorous stirring. The root is next filtered off while warm. It is afterwards dispersed in 400 mL of water, filtered, washed thoroughly with 500 mL of water, 150 mL of acetone then 500 mL of water and stored. The pure grafted co-polymer (PMMA-WHR) is then dried at 110 °C to constantly weigh, the grafting yield equal 95 %.

2.4. Preparation of solvent impregnated water hyacinth roots

Wet impregnation method was chosen for conducting the impregnation of TBP solvent onto either WHR or GWHR. The experiments were performed in 100 mL glass beaker using TBP (diluted with kerosene) and 5.0 g the pretreated dry roots. To verify the maximum impregnation, the major factors affecting the impregnation were studied at room temperature. After each impregnation experiment, the TBP remained was separated from the impregnated roots using plastic net, and its volume was determined. Samples from the solvent before and after impregnation were analyzed against its TBP concentration. The impregnated samples were well washed with distilled water to free the root beads from any adhered TBP and diluent, which can be assured by the disappearance of the solvent spots floating on the surface of the wash water. The washed impregnated root samples were then dried overnight in an oven at 50 °C. The dried mass was accurately determined then actual mass of the impregnated TBP was calculated.

2.5. Sorption isotherms

In isotherm studies, batch adsorption studies of uranium were performed at room temperature (25 °C). A series of 50 mL test tube was used; each one was filled with 25 mL of uranium leach liquor. Variation of the uranium concentrations of the leach liquor was obtained by dilution or by uranium spiking. The uranium concentration retained in the solid phase (mg/g) was calculated by:

$$q_e = (C_o - C_e)V/m \quad (1)$$

Where C_o and C_e are the initial and the equilibrium concentrations of the uranium) (mg/l), respectively, V is the volume of the aqueous solutions (L), and m is the weight of the sorbent (g).

The distribution of uranium between the solid, liquid interfaces at equilibrium has been studied by the Langmuir and Freundlich isotherm models. Langmuir isotherm equation may be written as:

$$C_e / q_e = (1/ b\, q_o) + (C_e / q_o) \quad (2)$$

Where q_e is the amount of solute sorbed per unit weight of adsorbent (mg/g), C_e is the equilibrium concentration of the solute in the bulk solution (mg/L), q_o is the monolayer adsorption capacity (mg/g) and b is the constant related to the free energy of adsorption. Freundlich equation may be written as:

$$\log q_e = \log K_f + 1/n \log C_e \quad (3)$$

Where K_f is the constant indicative of the relative adsorption capacity of the adsorbent (mg/g) and 1/n is the constant indicative of the intensity of the adsorption.

2.6. Kinetic studies

Pseudo first-order and second-order models were used in this study to explain the adsorption process.

2.6.1. Pseudo first-order kinetics

The adsorption rate is based on the adsorption capacity and acts according to the pseudo first-order equation as the following:

$$\log (q_e - q_t) = \log q_e - [k_{ad}\, t / 2.303] \quad (4)$$

Where; q_e and q_t are the amounts of the adsorbed uranium ions (mg/g) at the equilibrium time and at any instant of time "t," respectively, and k_{ad} is the rate constant of the pseudo first-order adsorption operation (l/min). Plotting of log $(q_e - q_t)$ versus t gives a straight line of the pseudo first-order kinetics [22, 23].

2.6.2. Pseudo second-order kinetics

The applicability of the pseudo second-order kinetics has to be tested for q_e estimation with equation given by:

$$t / q_t = 1/h + (1/q_e)\, t \quad (5)$$

Where; $h = k_2 q_e^2$ that can be regarded as the initial sorption rate as $t \rightarrow 0$. Under such circumstances, the plot of t/q_t versus t should give a linear relationship which allows the computation of q_e and k_2.

2.7. Chemical characterization methods

The chemical composition of the adsorbents (WHR, GWHR, TBP-WHR and TBP-GWHR) before and after uranium adsorptions was examined using wet chemistry methods. Total organic carbon (TOC) was determined using a Total Organic Carbon Analyzer TOC-5000 series combined with SSM-5000A (Shimadzu, Kyoto, Japan). Total carbon (TC) was detected in the samples by using the catalytically combustion oxidation at 900 ^{0}C, while inorganic carbon (IC) was analyzed in the samples after acidification at a temperature of 250 ^{0}C. TOC was calculated as a difference between TC and IC and was used for calculation of the polymer content in GWHR. The infrared spectra (IR) of water hyacinth root samples were obtained using a Fourier transform IR spectrophotometer Spectrum 2000 (Perkin Elmer) in order to determine the functional groups of the samples before and after uranium adsorption.

Morphology of the sample's surface was carried out by scanning electron microscopy (SEM LEO 1430 VP). To understand the swelling properties of the roots' samples a size distributions' measurements were carried out by using laser techniques.

3. Results and discussions

In their natural form, and before either the chemical grafting or the solvent impregnation, the water hyacinth roots surface is covered with inorganic and organic impurities. In general during chemical curing of roots, most of the surface impurities are removed, which makes the roots surface rough and improve the adhesion of the roots surface and either the polymer matrix or TBP.

3.1. Chemical characterization

3.1.1. Elemental analysis

Elemental analysis data of C, H, O and N shown in Table 2, were calculated from methods mentioned before. The samples are all carbon-rich, as is typical of WHR, and they have low ash and sulfur contents. Atomic nitrogen content is highest for GWHR and lowest for other samples. The metal contents of the roots showed in Table 3, which contains data for eight metals in the roots. The WHR has the highest levels of Ca, Cr, Cu, Fe, Mg, Na and Ni in its roots. Lower metal levels were observed in the corresponding samples, except for Na and Si, which persist in the roots even after impregnation or chemical grafting.

Table 2: Elemental analysis of water hyacinth root samples.

Element	WHR	GWHR	TBP-WHR	TBP-GWHR
	Conc. %	Conc. %	Conc. %	Conc. %
C	50.0	52.0	51.0	50.0
O	30.0	33.0	40.0	39..0
N	02.0	05.0	01.0	04.0
H	05.0	07.0	07. 0	04.00
S	0.30	0.10	0.10	0.05

Table 3: Metal analysis of water hyacinth root samples.

Element	WHR	GWHR	TBP-WHR	TBP-GWHR
	Conc. %	Conc. %	Conc. %	Conc. %
Si	12.0	02.0	00.9	01.00
Al	00.5	00.2	00.2	00.21
Fe	00.3	00.2	00.18	00.17
Cl	0.04	0.04	0.03	0.03
Na	0.02	0.013	0.01	0.01
K	00.1	0.05	00.04	00.03
Ca	00.1	0.07	0.09	0.02
Mg	0.04	0.02	0.01	0.01

3.1.2. Carbohydrate analysis

Table 4, shown the carbohydrate composition of water hyacinth root. It has been clear that all the percentages decreased after the chemical treatment.

Table 4: Carbohydrate composition of water hyacinth root samples.

Sorbents	Hemicellulose %	Cellulose %	Lignin %	Ash content %
WHR	16	28	15	17
GWHR	14	22	13	07
TBP-WHR	10	27	10	10
TBP-GWHR	12	20	10	08

3.2. Physical characterization

3.2.1. FTIR spectrum

The FTIR spectra of the studied sorbents (WHR, GWHR, TBP-WHR and TBP-GWHR) before uranium adsorptions are shown in Fig.1. In case of WHR, intense bands at 3697, 3621, 1631, 1103, 1015, 913, 796, 694, 537, 469 cm^{-1} (Fig. 1-A) were observed. The peak at about 1255 cm^{-1} is attributed to the lignin components [24], and the peak at 1517 cm^{-1} is within the typical region of aromatic ring C–C stretching [25]. Bands centered at about 2924 and 2854 cm^{-1} are assigned the asymmetric and symmetric C–H stretching of the aliphatic groups [26]. The band at 1720 cm^{-1} is attributed to the C-O stretching of the carboxylic group [27]. The peak at 1637 cm^{-1} is assigned C-O for stretching of carboxylate. The stretching vibrations of – OH at 3000–3700 cm^{-1} and the stretching vibrations of C–O at 1036 cm^{-1}demonstrated the presence of alcoholic hydroxyl groups [28]. After grafting with PMMA the aforementioned bands have preserved, but new bands of polymer groups, 2920, 2851, 1471 cm^{-1} (Fig. 1-B) have appeared [29]. Also, after impregnation of either the natural or the grafted roots with TBP the aforementioned bands have preserved, but new bands of TBP groups, 2920, 2851, 1471 cm^{-1} (Fig. 1-C, 1-D) have appeared. Compared FTIR spectra of the studied roots, within uranium loaded roots shown in Fig. 2 (A, B, C and D) which displayed a significant shift in some of the peaks. The shift of the 3414 cm^{-1}peak to 3417 cm^{-1} suggests the attachment of uranium on –OH group. The shift of the peak at 1637 to 1645 cm^{-1} reflects the changes in the stretching frequency of carboxylate upon binding of uranium. Moreover, two bands of small intensity are observed at 2927 and 2857 cm^{-1}, this can be assigned to UO_2^{2+} [30]. According to Vidya *et al*. [31], the uranyl ions' adsorption on mesoporous molecular sieves leads to appearance of bands of small intensity at 902 cm^{-1} (U = O), 915-833 cm^{-1} (O=U=O). It was observed the same bands in our study for the root samples with the uranium loading. The IR bands appearing in 1525 and at 1379 cm^{-1} in the spectra corresponded to U connecting with

organic TBP. These observations confirm the complex formation between the adsorbent and the uranium.

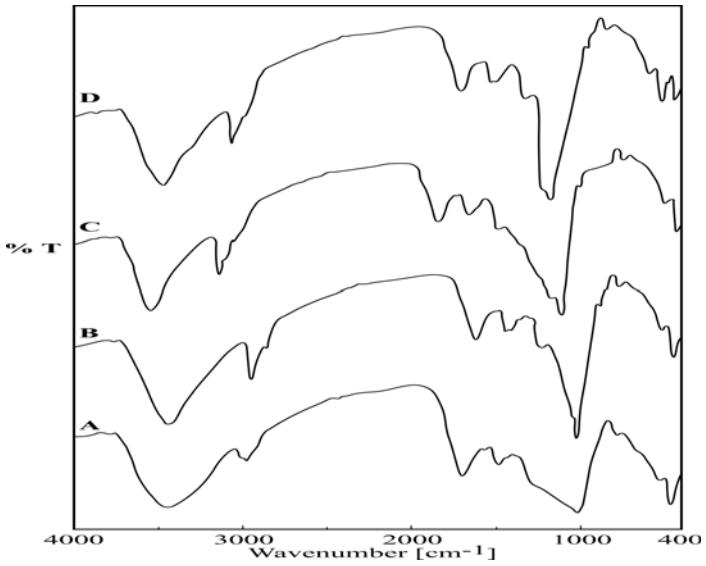

Fig 1: FTIR spectra of roots before uranium adsorption. (A. WHR, B. GWHR, C. TBP-WHR and D. TBP-GWHR)

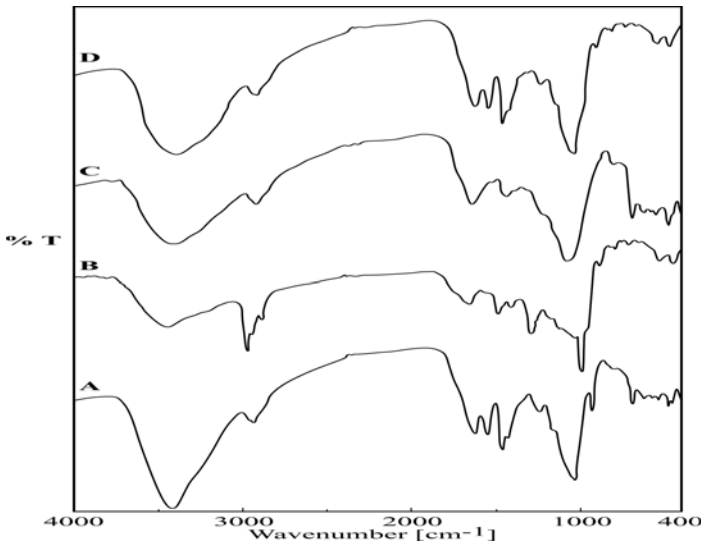

Fig 2: FTIR spectra of roots after uranium adsorption. WHR, B. GWHR, C. TBP-WHR and D. TBP-GWHR)

3.2.2. Scan electron microscope (SEM)

Microphotographs of water hyacinth root samples before adsorption are presented in Fig. 3. The microphotographs show that the well-preserved forms of WHR generally have cylindrical and plate shapes with well-developed porous structure. There are also small broken particles of other kinds. As one can see in Fig. 3A, the centric diatom is approximately 50 µm radius and 10 µm thickness. The body of these roots is covered with clean pores for 500–700 mm in diameter. The grafted roots' particles have a cylindrical shape of a 7–15 µm in stretch and 10 –15 µm in external diameter (Fig. 3B). The thickness of grafted roots cylinders is about 5 µm and their surface is also covered with pores of 350 – 400 mm in diameter. Moreover, the walls of the cylinders are folded by a few circular belts. The characteristics of the impregnated samples (Fig. 3C, 3D) shows that the porous structure of this material may be successfully modified by the organic TBP phase. The thickness of impregnated roots cylinders is about 15 - 20 µm and their surface is also covered with pores of 600 – 850 mm in diameter. Compared with SEM of the studied roots, SEM of uranium loaded roots are shown in Fig. 4 (A, B, C and D) which show that the walls of the cylinders is covered by cluster forms of the uranium. The clusters sizes range from 2 to 7 micrometers in size.

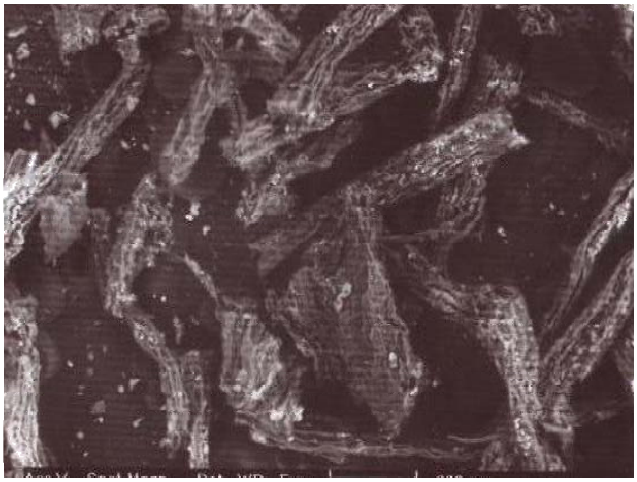

Fig 3A: SEM of WHR before uranium adsorption.

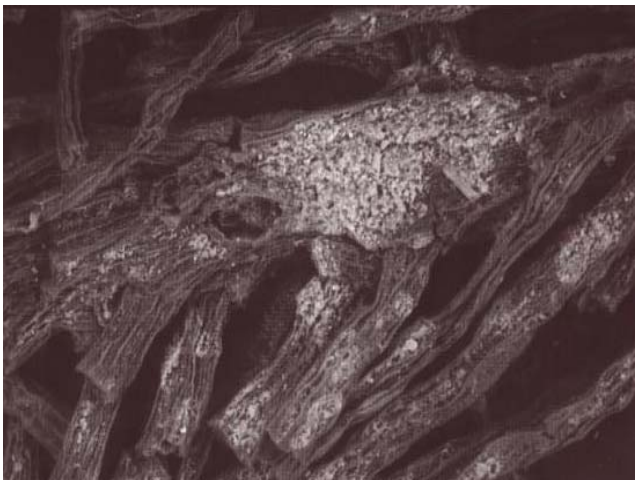

Fig 3B: SEM of GWHR before uranium adsorption.

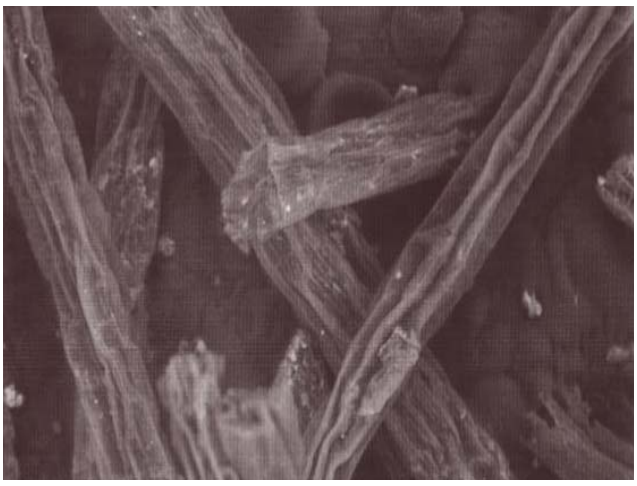

Fig 3C: SEM of TBP-WHR before uranium adsorption.

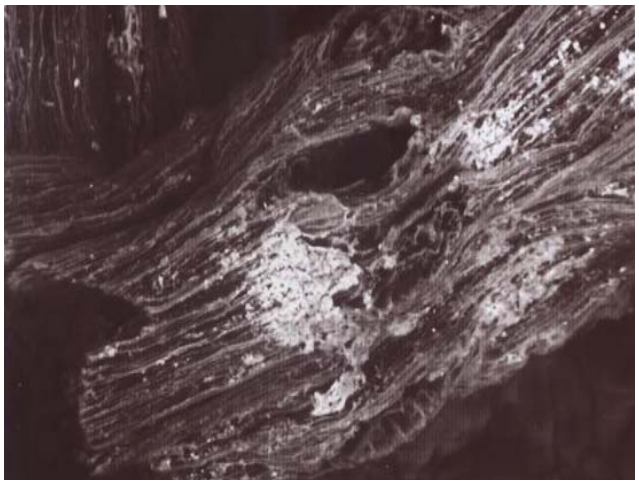

Fig 3D: SEM of TBP-GWHR before uranium adsorption**.**

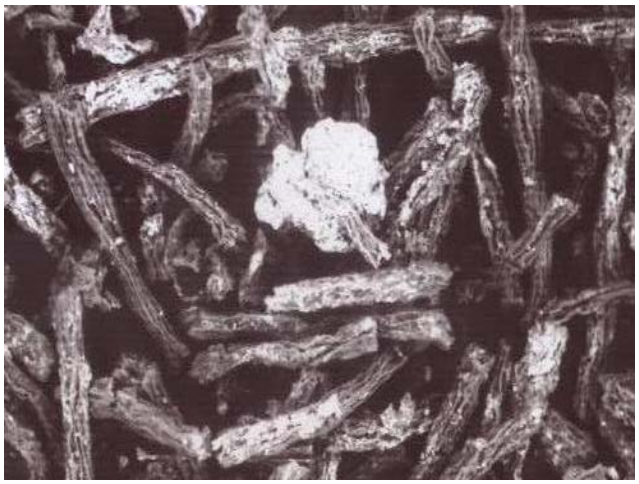

Fig 4A: SEM of WHR after uranium adsorption**.**

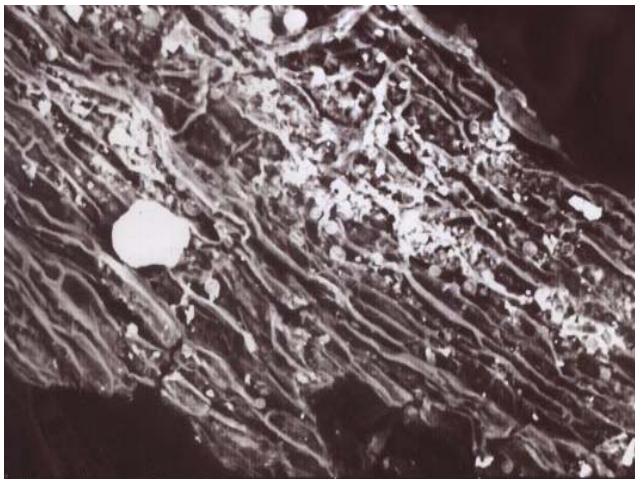

Fig 4B: SEM of GWHR after uranium adsorption.

Fig 4C: SEM of TBP-WHR after uranium adsorption**.**

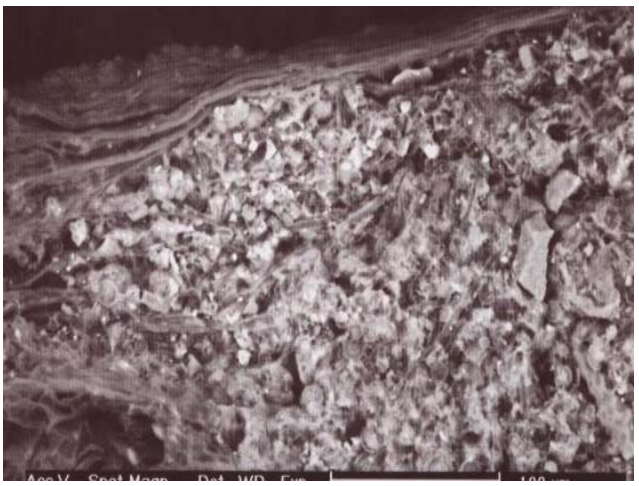

Fig 4D: SEM of TBP-GWHR after uranium adsorption.

3.2.3. Size distribution

Zeta potential measurements are widely used for the determination of the particle size of a variety of different solid materials. The zeta potential measurements of the studied samples show that the impregnated roots have a bigger particle size than the other ones as shown in Fig. 5.

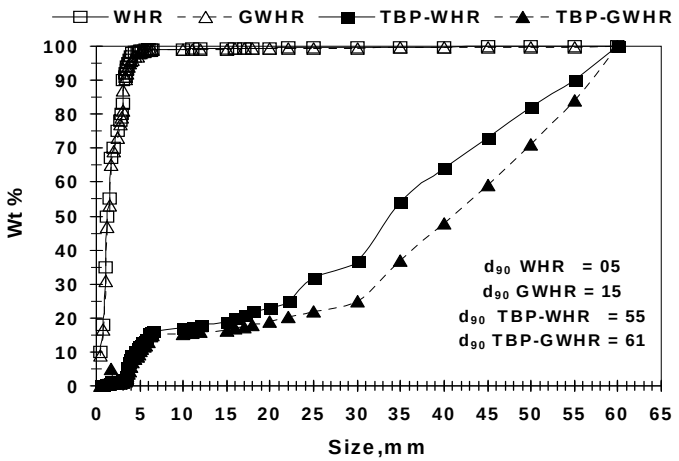

Fig 5: Size distribution of WHR, GWHR, TBP-WHR and TBP-GWHR.

3.3. Impregnation studies

The results of the investigated factors affected on the impregnation efficiency % will be discussed here, which involve solvent concentration, contact time, diluent and the solid liquid phase ratio.

3.3.1. Effect of TBP concentration

Figure 6 shows the effect of TBP concentration on the impregnation efficiency of WHR and GWHR. The data revealed that the impregnation efficiency was gradually increased to 50 and 90% by increasing the concentration of TBP in kerosene to 20% (v/v) for WHR and GWHR, relatively. The maximum impregnation efficiency reached 50 and 150% for WHR and GWHR, respectively, when the undiluted TBP was used. The maximum impregnated amount of TBP by GWHR is higher by 16% than that impregnated using Amberlite XAD - 4, which was only 1.26 g/g [32].

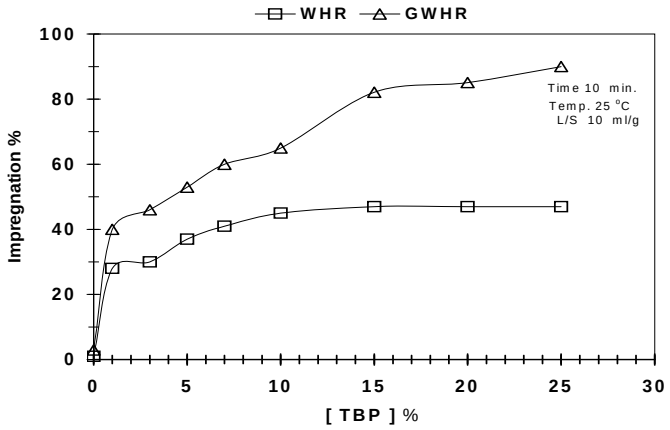

Fig 6: Effect of TBP concentration on the impregnation %.

3.3.2. Effect of contact time

The effects of contact time on TBP impregnation efficiency onto WHR and GWHR were studied to attain the equilibrium time for maximum impregnation. The results are shown in Fig. 7. Clearly the impregnation of TBP solvent proceeds rapidly from the first 10 min. Where it reached 10% and 50% for WHR and GWHR, respectively, and increased steadily to reach the maximum value of 50% and 90% for WHR and GWHR, respectively after 30 minutes.

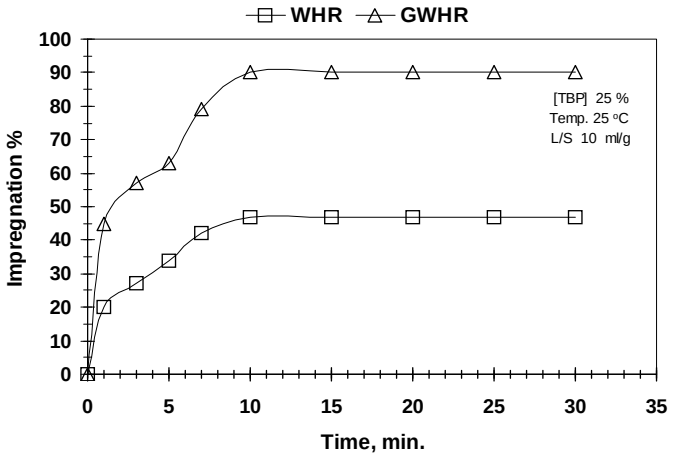

Fig 7: Effect of contact time on the impregnation %.

3.3.3. Effect of diluents

The diluent effect upon the impregnation % of the roots by TBP was studied using different diluents (Ethanol, Propanol, 1-octanol, Cyclohexane, Benzene, Kerosene and Toluene). Experimental data represented in Table 5 shows that the Kerosene gave the highest impregnation efficiency compared to the other solvent.

Table 5: Effect of diluents on TBP impregnation % of the roots.

Sorbent / Diluent	Impregnation %	
	WHR	GWHR
Kerosene	50	90
Ethanol	40	79
Propanol	41	81
1-octanol	42	80
Cyclohexane	48	87
Benzene	51	92
Toluene	50	91

3.3.4. Effect of phase ratio

The effect of the liquid, solid ratio (L/S) on impregnation efficiency was studied as shown in Fig. 8. The results showed that, in case of WHR the impregnation efficiency slightly increased from 30 to 50 by increasing the (L/S) ratio from 10 to 30. In case of GWHR the impregnation efficiency quite increased from 40 to 90 by increasing of the (L/S) ratio from 10 to 30. However, the impregnation efficiency of GWHR higher than that of WHR, reflecting the hydrophobic character of GWHR surface.

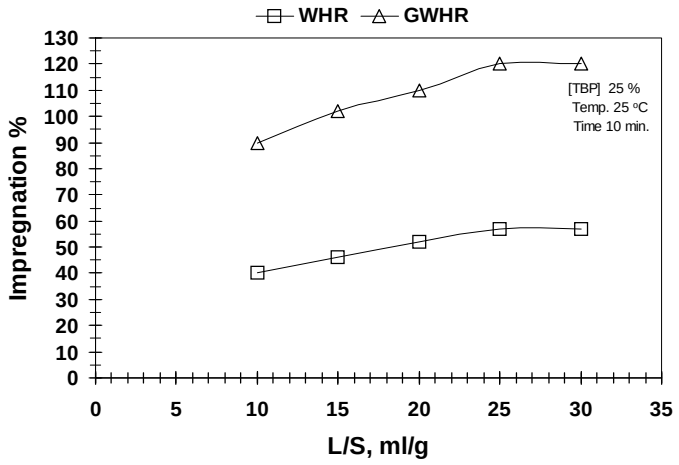

Fig 8: Effect of L/S phase ratio on the impregnation %.

3.4. Sorption studies

3.4.1. Effect of pH

Hydrogen ions affect the surface charge of adsorbents, and the adsorbed species [33-35]. As H^+ is a known competing species in cation exchange processes, the effect of media pH on the adsorption capacity of roots was studied. The effects of pH on the uranium adsorption onto WHR, GWHR, TBP-WHR and TBP-GWHR were investigated using 20 mL of 500 mg/L uranium leach liquor solution, for a pH range of 1.0-8.0 at 25 °C for 10 minutes. The uranium adsorption capacities (q_e) of WHR, GWHR, TBP-WHR and TBP-GWHR were greatly affected by the solution pH variations as shown in Fig. 9. The adsorption capacity increased with pH rising up to pH 5.0 and then declines slowly with a further rise in pH. In strongly acidic solutions, more protons will be available to proton-ate phenolic and carboxylic groups on the root surface, reducing the number of binding sites for the adsorption of UO_2^{2+}; therefore, the adsorption capacity of uranium is lower in acidic solutions (pH < 5.0). However, the increasing of pH value beyond 5.0; hydrolysis precipitation starts due to the formation

of complexes in aqueous solution, decline of uranium (VI) adsorption capacity [36, 37]. Furthermore, it was noticed that the impregnated roots either the natural or the grafted has the higher adsorption capacity than the non-impregnated one due to it was believed that the uranium adsorption occurred via its interactions with functional groups of TBP.

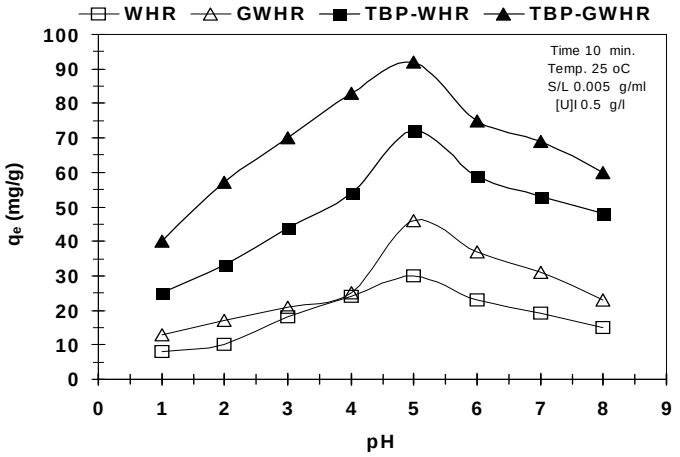

Fig 9: Effect of pH on the uranium sorption.

3.4.2. Effect of contact time

Under conditions of, an adsorbent amount of 0.1 gm, pH 5.0, temperature 25 ˚C and 500 mg/L uranium leach liquor, the adsorption experiments for WHR, GWHR, TBP-WHR and TBP-GWHR were investigated over time intervals from one up to 30 minutes. Figure 10 illustrates the data obtained showing that the adsorption of uranium was proceeding rapidly. It closely reached a maximum after 10 minutes, and nearly remained constant up to 30 minutes. Rapid uranium adsorption, which is similar to the adsorption of other metals [38], was contributed significantly to equilibrium uptake, which is interpreted to be the instantaneous adsorption stage or external surface adsorption. After 10 minutes, there are no notable effects on the uranium adsorption capacities so, 10 minutes was considered the adsorption.

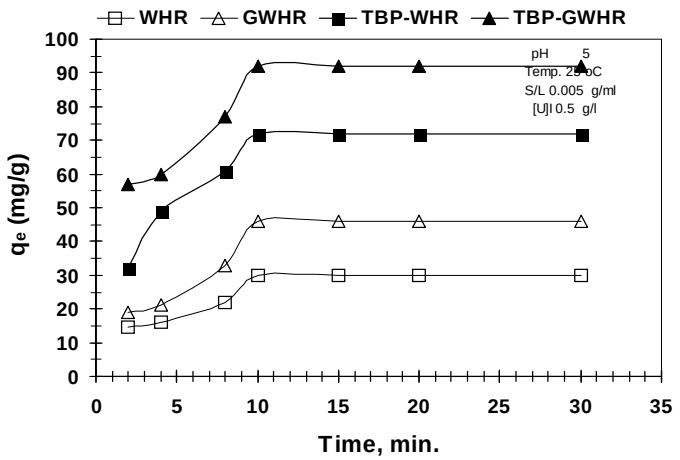

Fig 10: Effect of contact time on the uranium sorption.

3.4.3. Sorption isotherm

The effect of the original uranium concentration on the adsorption capacity of the roots (WHR, GWHR, TBP-WHR and TBP-GWHR) was studied using a range of initial uranium concentrations, 0.1 to one gm/L. The results are shown in Fig. 11, clearly that, the adsorption capacity of uranium increased with rising the initial uranium concentration in the aqueous solution; this is because more mass of uranium is put into the system by increasing the initial uranium concentration in the solution at the same amount of adsorbent [39].

The adsorption experimental data were subjected to analysis according to the Langmuir isotherm by plotting C_e/q_e vs. C_e as shown in F.g. 12, which gives a straight line with intercept and slope values equal to 1/bqo and 1/qo, relatively. Moreover, Freundlich isotherm was applied from the adsorption data by plotting log q_e vs. log C_e giving a straight line with slope and intercepts values equal to 1/n and log K_f, correspondingly, as shown in Fig. 13. The isotherm data for the uranium adsorption was calculated from the slopes and intercepts of figures 12 and 13 and reported in table 6.

The values of the constant (b) for the treated roots are higher than that for the natural roots. Higher (b) values refer to stronger interaction between uranium and the active sites of the adsorbent [40].

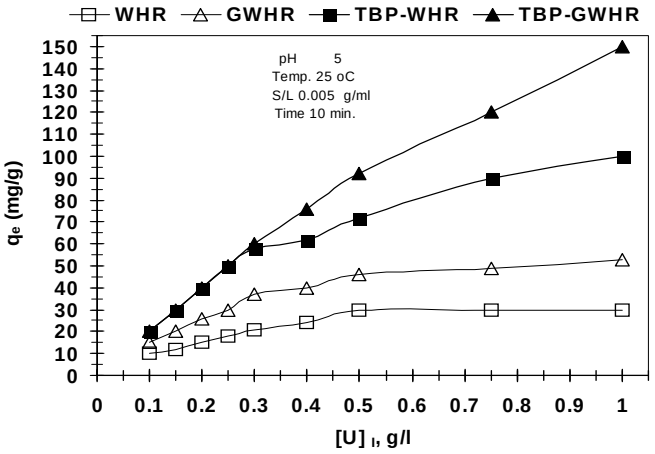

Fig 11: Effect of initial concentration on the uranium sorption.

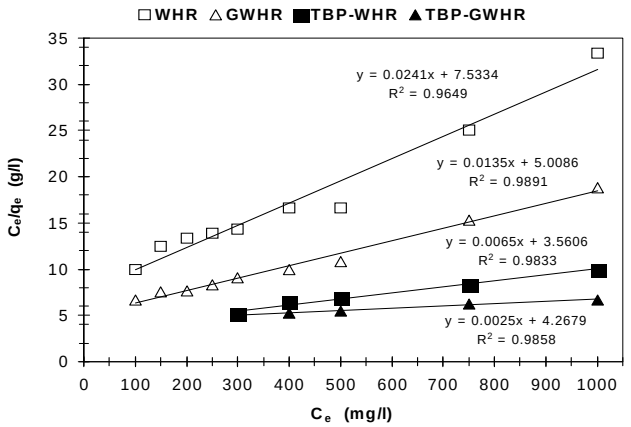

Fig 12: Langmuir isotherm of the uranium sorption.

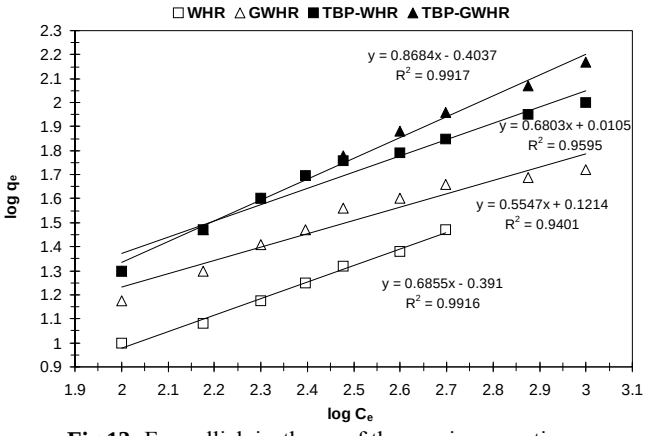

Fig 13: Freundlich isotherm of the uranium sorption.

Table 6: Isotherm data of uranium adsorption.

Sorbent	Isotherm data			
	Langmuir		Freundlich	
	q_o (mg/g)	b	1/n	log K_f
WHR	42	0.003	0.68	0.39
GWHR	74	0.0027	0.55	0.12
TBP-WHR	153	0.0018	0.68	0.01
TBP-GWHR	400	0.0005	0.86	0.40

3.4.4. Effect of temperature

The effects of temperature on the adsorption of uranium by WHR, GWHR, TBP-WHR and TBP-GWHR were studied from 25 to 50 °C. The results shown in Fig. 14 revealed that, there is no significant change in the adsorption capacity of uranium, with temperature variation, indicating that the process is spontaneous in nature.

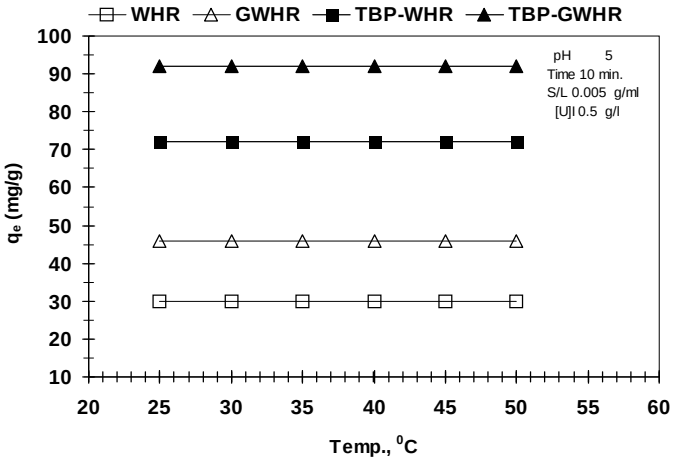

Fig 14: Effect of temperature on the uranium sorption.

3.4.5. Sorption kinetics

In order to determine the kinetic parameters and explain the mechanism of the adsorption processes, many researchers have used first and pseudo second-order rate expressions [41]. The uranium adsorption data by WHR, GWHR, TBP-WHR and TBP-GWHR were subjected to analysis according to the first-order equation by plotting log ($q_e - q_t$) versus time as shown in Fig. 15. The adsorption rate constants (k_1) can be determined experimentally from the obtained straight line. The rate constants and r^2 values of the kinetic models are shown in Table 6. The experimental data give a good fit for root samples (r^2~0.96) indicating that the pseudo first-order model is applicable for WHR, GWHR, TBP-WHR and TBP-GWHR. Furthermore, pseudo second-order model was applied from the adsorption data by plotting t/q_t versus time (t) as shown in Fig. 16. The rate constant (k_2), and q_e are given from the figure and reported in Table 7. Based on the obtained correlation coefficients (r^2), the experimental data of the roots conformed better to the pseudo-second-order equation, evidencing chemical adsorption involving valence forces through the sharing or exchange of electrons between adsorbent and adsorbate [42] as a rate-limiting step of the adsorption mechanism [43].

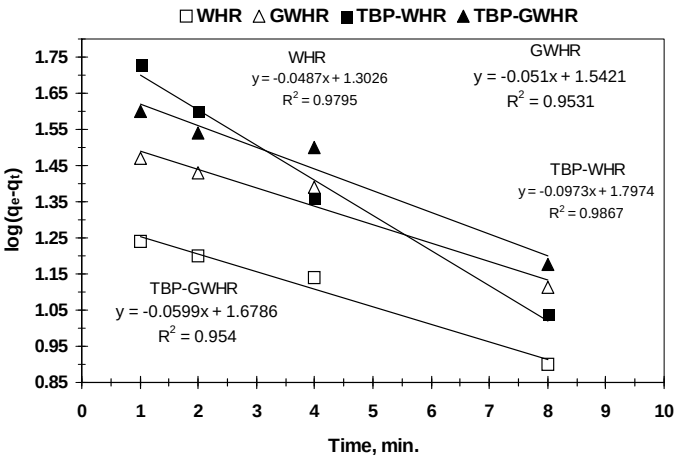

Fig 15: Pseudo first - order model for the uranium sorption.

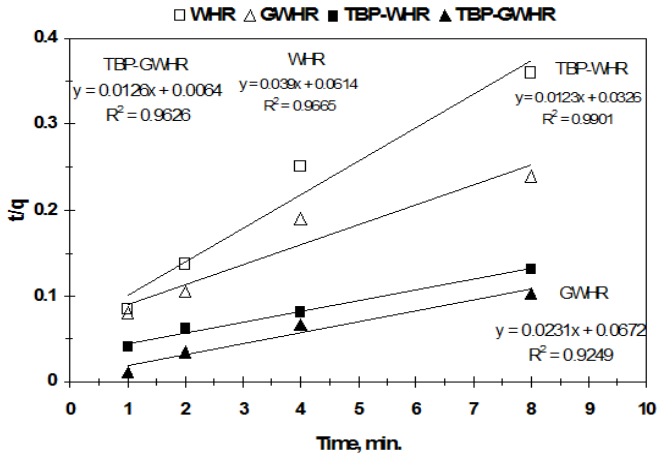

Fig 16: Pseudo second - order model for the uranium sorption.

Table 7: Kinetic data of uranium adsorption.

Sorbent	Kinetic data					
	Pseudo first - order			Pseudo second - order		
	k_1	log q_e	r^2	k_2	q_e	r^2
WHR	0.048	1.30	0.97	0.189	25	0.96
GWHR	0.051	1.54	0.95	0.037	43	0.92
TBP-WHR	0.097	1.79	0.98	0.029	81	0.99
TBP-GWHR	0.059	1.67	0.95	0.029	79	0.96

3.4.6. Effect of interfering ions

The effects of interfering ion's presence on the adsorption of uranium by WHR, GWHR, TBP-WHR and TBP-GWHR were studied as shown in Table 8. In this respect, the adsorption of uranium was performed first in the absence of any interfering ions to observe any changes. Major and trace element's standard concentration of 250 mg/L were prepared because they were composing the matrix of the most geologic samples and present in the laboratories effluents waste water streams. These experiments are carried out by maintaining the initial uranium concentration, pH, and S/L constant at 500 mg/L, 5, and 0.05 g/mL, respectively at room temperature for 10 minutes. The results revealed that, there is no significant effect was recorded by the interfered ions except for iron and thorium; however, the effect is minimized in the case of the impregnated roots (TBP-WHR, TBP-GWHR).

Table 8: Effect of interfering ions on uranium adsorption uptake.

Sorbent / Interfering Ions	Uranium uptake capacity, q_e (mg/g)			
	WHR	GWHR	TBP-WHR	TBP-GWHR
--------	30	46	72	92
NH_4	29	41	71	92
Na^+	26	39	72	91
K^+	26	44	72	91
Fe^{3+}	09	31	67	85
P_2O_5	17	34	65	83
Co^{2+}	20	40	70	90
Ni^{2+}	21	41	70	89
Cu^{2+}	21	37	70	88
Zn^{2+}	19	30	71	87
Th^{4+}	18	27	61	82
SO_4^{2-}	14	26	65	81
V^{5+}	25	40	72	89
Al^{3+}	23	41	71	92
Si^{4+}	29	45	72	92
NO_3^-	17	29	68	89
Cl^-	16	28	67	87
Ca^{2+}	16	29	72	92
Mg^{2+}	17	31	72	92

3.5. Uranium desorption

The different eluents used for uranium desorption from WHR, GWHR, TBP-WHR and TBP-GWHR was investigated as shown in Fig. 17. It was found that HNO_3 is the most effective one for uranium desorption even at low concentration reached.

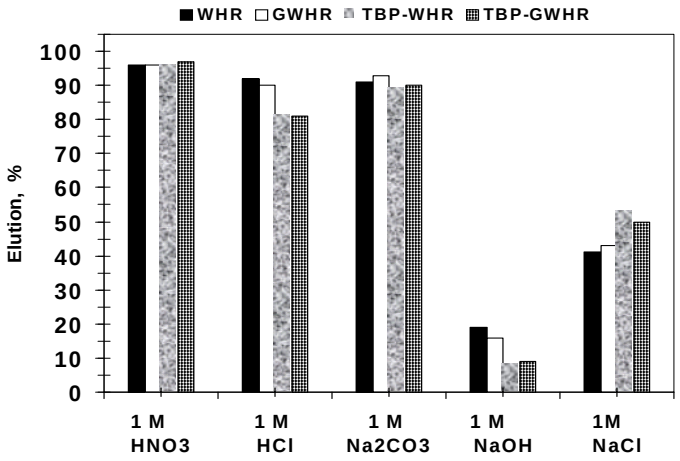

Fig 17: Uranium desorption by different eluents

4. Conclusion

The results obtained from this study lead to the following conclusions; 1- the optimum pH for uranium adsorption by WHR, GWHR, TBP-WHR and TBP-GWHR is pH 5, 2- the experimental data can fit satisfying both Langmuir and Freundlich model, 3- the uptake data of WHR, GWHR, TBP-WHR and TBP-GWHR can fit satisfying both pseudo first-order and pseudo second-order model, 4- the chemical grafting of the water hyacinth roots with polymethyl methacrylate (PMMA) increases the hydrophobic character of its surface and hence increasing the impregnation %, 5- the impregnation of the water hyacinth roots either the natural or the grafted with TBP enhanced the uranium adsorption capacity more much better and, 6- the adsorption capacity is found to be 42, 74, 153 and 400 mg g^{-1} for WHR, GWHR, TBP-WHR and TBP-GWHR, respectively.

5. References

1. Nishikido JJ, Katz GT, Seaborg, Morss LR. The Chemistry of the Actinide Elements, Chapman and Hall, London, 1986.
2. Yusan SD, Akyil S, Hazard J. Mater 2008; 160:388–395.
3. Goncharuk VV, Kornilovich BY, Pavlenko VM, Babak MI, Pshinko GN, Pysmennyi BV. J Water Chem Technol 2001; 23:44–50.
4. Yu B, Kornilovich IA. Kovalchuk GN, Pshinko EA, Tsapyuk AP, Krivoruchko. J Water Chem Technol 2000; 22:43–47.
5. Chang HS, Korshin GS, Wang Z, Zachara JM. Environ Sci Technol 2006; 40:1244–1249.
6. Aytas S, Akyil S, Eral M. J Radioanal Nucl Chem 2004; 260:119–125.
7. Vidya K, Gupta NM, Selvam P. Mater Res Bull 2004; 39:2035–2048.
8. Akyil S, Aslani MAA, Eral M. J Radioanal Nucl Chem 2003; 256:45–51.
9. Sabarudin A, Oshima M, Takayanagi T, Hakim L, Oshita K, Gao YH. Anal Chim Acta 2007; 581:214–220.
10. Aytas S, Yurtlu M, Donat R. J Hazard Mater 2009; 172:667–674.
11. Humelnicu D, Drochioiu G, Popa K. J Radioanal Nucl Chem 2004; 260:291–293.
12. Sprynskyy M, Kovalchuk I, Buszewski B. Journal of Hazardous Materials 2010; 181:700–707.
13. Sadeek S.A, Farag N.M, Kouraim M.N, Gado M.A. International Journal of Advanced Research 2014; 2:409-423.
14. Ghabbour AE, Davies G, Yam-Yuen L, Vozzella EM. Environmental Pollution 2004; 131:445-451.
15. Saha B, Gill RJ, Bailey DG, Kabay N, Arda M. J Reactive and Functional Polymers 2004; 60:223−244.
16. Kauczor HW, Meyer A. J Hydrometallurgy 1978; 3:65−73.
17. Kedari CS, Pandit SS, Ramanujam A. Journal of Radioanalytical and Nuclear Chemisty 1997; 222:141−147.
18. Kroebel R, Meyer A. Application of newly developed materials for extraction chromatography of inorganic salts in columns [C]/ Proceeding of the International Solvent Extraction Conference, ISEC74. London: Society of Chemical Industry, 1974, 2095.
19. Alcock K, Grimley SS, Healy TV, Kennedy J, Mckay HAC. Transactions of the Faraday Society 1956; 52:39−47.
20. Kumar S, Koganti SB. NUCL TECH, 2000; 129:279-283.
21. Marczinco Z. Spectrophotometric Determination of Elements, John Wiley and Sons Inc., New York, 1986.
22. Glasston S, Laidler KJ, Eyring H. The Theory of Rate Processes: the kinetics of chemical reactions, viscosity, diffusion and electrochemical phenomena, McGraw-Hill, New York, 1941.
23. Ruthven DM. Principles of Adsorption and Adsorption Processes, John Wiley& Sons Ltd. New York, 1984.
24. Fiol N, Escudero C, Villaescusa I. Bioresour Technol 2008; 99:5030–5036.
25. Liu CC, Wang MK, Chiou CS, Li YS, Lin YA, Huang SS. Ind Eng Chem Res 2006; 45:8891–8899.
26. Toupin M, Belanger D. Langmuir 2008; 24:1910–1917.
27. Southichak B, Nakano K, Nomura M, Chiba N, Nishimura O. Phragmites australis, Water Res 2006; 40:2295–2302.
28. Lim SF, Zheng YM, Zou SW, Chen JP. Environ Sci Technol 2008; 24:2551-2556.
29. Jung Y, Kim S, Park SJ, Kim JM. Colloids and Surfaces A: Physicochem, Eng. Aspects 2008; 314:292–295.
30. Sharma P, Tomar R. Micropor Mesopor Mater 2008;

116:641–652.
31. Aytas S, Akyil S, Eral M. J Radioanal Nucl Chem 2004; 260:119–125.
32. Khawassek YM. Modification of the purity of the extracted material from the radioactive mineral resources [PhD]. Egypt: Faculty of Engineering, Alexandria University, 2008.
33. Kula I, Ugurlu M, Karaoglu H. Celik A. Bioresour Technol 2008; 99:492–501.
34. Gupta VK, Rastogi A, Saini VK, Jain N. J Colloid Interf Sci 2006; 296:59–63.
35. Gupta VK, Rastogi A. J Hazard Mater 2008; 153:759–766.
36. Alvarez-Merino MA, Fontecha-Camara MA, Lopez-Ramon MV, Moreno-Castilla C. Carbon 2008; 46:778–787.
37. Hueso JL, Espinos JP, Caballero A, Cotrino J, Gonzalez-Elipe AR, Carbon 2007; 45:89–96.
38. Low KS, Tai CKCH. J Environ Sci Health 1994; 29:171-176.
39. Kütahyalı C, Eral M. Separation and Purification Technology 2004; 40:109–114.
40. Boonamnuayvitaya V, Chaiya C, Tanthapanichakoon W, Jarudilokkul S. Separation and Purification Technology 2004; 35:11–22.
41. Erdem M, Ozverdi A. Sep Purif Technol 2006; 51:240–246.
42. Jiménez-Cedillo MJ, Olguí CH, Fall MT. J Hazard Mater 2009; 163:939–945.
43. Song Wang X, Ping Tang Y, Rong Tao S. Chem Eng J 2009; 148:217–225.